DOI: 10.13009/EUCASS2025-653
11TH EUROPEAN CONFERENCE FOR AERONAUTICS AND SPACE SCIENCES (EUCASS)

A Feature-Based Data-Driven Approach for State-of-Health Estimation of Satellite Lithium-ion Batteries

Roberto Giovanni Sbarra[⋆†], *Michele Pasquali*[⋆], *Giuliano Coppotelli*[⋆], *Paolo Gaudenzi*[⋆],
Davide di Ienno[§], *Niccolò Picci*[§], *Carlo Ciancarelli*[§]
[⋆]*University of Rome "La Sapienza",* [§]*Thales Alenia Space Italia S.p.A.*
robertogiovanni.sbarra@uniroma1.it
[†]Corresponding author

Abstract

The present work introduces a data-driven framework for evaluating the SOH of lithium-ion batteries used in satellites, addressing the unique challenges posed by the space environment. A robust methodology is proposed for indirect SOH estimation based on optimal health indicator (HI) extraction. By leveraging correlation analysis, feature redundancy is minimized and its relevance to capacity prediction is maximized. This approach facilitates the generation of an optimal set of features that ultimately enhances the accuracy of the SOH prediction framework. The feasibility and validity of the proposed methods are demonstrated using a lithium-ion battery test dataset from the NASA prognostic center.

1. Introduction

Lithium-ion batteries have revolutionized the energy storage landscape with their high-energy density, long cycle life, and low self-discharge rates. Their adoption in spacecrafts and satellites marks the advent of the third generation of space energy storage, playing a pivotal role in ensuring the operation of satellite subsystems.[1]
Despite their excellent performance, lithium-ion batteries are not immune to electrochemical degradation, leading to reduced capacity, reliability issues, and even catastrophic mission failures.[2] Irreversible electrochemical reactions (e.g., lithium deposition, electrolyte decomposition, active material loss) during the charging and discharging phase cause performance degradation in rechargeable batteries as Li-ion batteries, impacting the reliability of battery energy storage systems.[3] Therefore, prognostics and health management are critical for improving the reliability of Li-ion batteries in satellite systems.
The State Of Health (SOH) is commonly defined as the ratio of actual capacity to nominal capacity. The actual capacity estimation is widely used in many applications to evaluate the degradation process of Li-Ion batteries. Despite its power in representing the degradation state of Li-Ion cells, capacity measurement is time-consuming and requires expensive instruments, making it challenging to use in real-time applications such as space missions.[4]
The dynamic operative profiles and the extreme conditions typical of space missions create a unique challenge in the SOH estimation, highlighting the need for innovative and robust solutions.[5] Various SOH techniques have been proposed in recent years. A consistent part of these works is based on the extraction of representative Health Indicators (HIs), directly from the battery observables (current, voltage and temperature). These indicators provide valuable information about the degradation process of Li-ion cells, demonstrating a strong correlation with capacity. This virtual sensing approach has been extensively used in SOH estimation. In,[6] it is a comparative analysis that involve different Deep Learning techniques based on time series and extracted His. The study demonstrates that the features are more suitable for most situations, since the complete charging data or partial charging data may contain more noise. Different approaches are based on data-driven methods employed to learn the relation between the capacity and indicators extracted from the voltage curve,[7,8] current curve,[9] and the temperature, both in the charge and discharge phase.[10] Furthermore, the combined use of HIs extracted from multiple observables has been demonstrated to yield improved performance.[11] In the framework of the HI-based approach, some authors focus on optimizing the performances of the indicators using the Principal Component Analisys (PCA) in order to reduce the dimensionality of the extracted HIs, avoiding overfitting problems, reducing the burden of computation, and optimizing the feature selection.[12,13]
The aim of this work is to extract the most representative features from the available observables using a pre-processing approach, providing a robust and efficient representation of the degradation pattern present in the data. Principal component analysis (PCA) is employed to summarise the different indicators extracted from current, voltage and temperature measurements in the charge phase. Correlation analysis is performed to understand the relationships between the HIs

Copyright © 2025 by University of Rome "La Sapienza" and Thales Alenia Space Italia S.p.A., Published by the EUCASS association with permission.

DOI: 10.13009/EUCASS2025-653

and the SOH, and between the HIs themselves. Furthermore, feature importance analysis using cross-validation testing was employed to observe how the contribution of the HIs to the solution is affected by different operating conditions. Finally, a feedforward neural network (FNN) is trained and validated to provide a robust, general tool for estimating SOH. To assess the feasibility and reliability of the proposed approach, validation is performed using a lithium-ion battery dataset from NASA's Prognostic Centre.

2. Theoretical background

2.1 Correlation Coefficients

The Pearson Correlation Coefficient is a statistical measurement of linear Correlation between two variables.[14] The Equation 1 gives the Pearson correlation coefficient between two variables x and y:

$$\rho = \frac{\sum_{i=1}^{n}(x_i - \bar{x})(y_i - \bar{y})}{\sqrt{\sum_{i=1}^{n}(x_i - \bar{x})^2}\sqrt{\sum_{i=1}^{n}(y_i - \bar{y})^2}} \tag{1}$$

where x_i and y_i are the variables at the i-th observation, $\bar{y}$ and $\bar{x}$ the mean values, and n is the number of observations. The Pearson coefficient is defined in the range [-1,1]: the higher the relation between the variables, the closer the absolute value of ρ to 1.

2.2 Principal Component Analysis

The Principal Component Analysis (PCA) is a method employed in dimensionality reduction based on the variance of the data.[15] This method allows the transformation of the data into a new coordinate space with a lower dimension. Through an orthogonal transformation, a set of linearly correlated variables is converted into a set of linearly uncorrelated variables. The principal components are given by the most relevant eigenvectors (largest eigenvalues) of the covariance matrix. Leveraging the singular value decomposition (SVD) of the mean-centered data matrix, it is possible to efficiently compute the principal components that reflect the relevant part of the variance present in the original data.

2.3 Random Forest

Random Forest (RF) is one of the most widely used ensemble learning algorithms for both classification and regression tasks.[16] It builds a collection of decision trees, which act as weak learners, and combines their predictions to form a more accurate and robust model. This ensemble approach significantly reduces overfitting and improves generalisation compared to using a single decision tree. RF integrates two key ideas to overcome the limitations of individual decision trees:

- Bagging: Each tree is trained on a random sampling of the training data, allowing the reduction of the variance of the model by introducing diversity in the training subsets.
- Random Feature Subset Selection (Random Node Split): At each split in the tree, only a random subset of features is considered. This strategy reduces the correlation among trees, enhancing the generaliszation ability.

An important built-in capability of RF is its ability to compute feature importance, which is crucial for feature selection in statistical models. RF can be seen as implementing a wrapper method for feature selection, where the learning algorithm itself (i.e., the random forest) is used to score and rank features based on their predictive power.

2.4 Feedforward Neural Network

The Feedforward Neural Network (FNN) is a supervised machine learning technique consisting of interconnected layers of neurons which maps the nonlinear relation between an input vector and an output vector. Generally, a FNN consists of an input layer that passes the input vector to the network, one or more fully connected hidden layers (each node is connected to every node in the next and previous layer) and finally an output layer.[17] At the neuron level, the output is carried out by a nonlinear activation function of the weighted input, Equation 2,[18]

$$y = \phi(W \cdot x + b) \tag{2}$$

where $\phi(\cdot)$ represents the activation function, W is the weight matrix, b denotes the bias vector, and x is the input vector. The output of each node is scaled by the connecting weight, transformed by a nonlinear activation function

DOI: 10.13009/EUCASS2025-653

and fed forward to be an input to the nodes in the next layer of the network. By a superposition of many nonlinear transfer functions, the FNN can approximate extremely non-linear functions. The weights and bias at each node are learned from a training dataset, which consists of a series of input and associated output vectors. During training, a predefined cost function, defined between the desired and actual output, is evaluated at each iteration weights and bias in the network are optimally adjusted to minimize this function. Once trained with suitably representative training data the Feedforward Neural Network can generalize to new, unseen input data.

3. Analisys and Results

3.1 NASA Dateset

The NASA Ames Prognostics Center of Excellence (PCoE)[19] dataset is composed of laboratory test carried out on different sets of 1850 commercial Li-Ion cells.Each set of cells differs from the others due to the varying operating conditions applied during the test The Constant Current (CC), Constant Voltage (CV) charge mode is common for all the cells. In the CC phase the current is fixed at 1.5 Ampere until the voltage reaches the cut-off value of 4.2 V. Then the CV phase is used until the current drops to 0.02 Ampere. In all the charge process the battery terminal voltage, battery output current and battery temperature are recorded.
On the other hand, the discharging phase is performed differently for each set of cells, leveraging constant current, square wave loading and multiple load current levels. During the discharge, the battery terminal voltage, battery output current and battery temperature and capacity are recorded. Repeated charge and discharge cycles result in accelerated aging of the batteries, allowing the use of this dataset for SOH estimation and the prediction of the remaining useful life (RUL).The experiments were stopped when the batteries reached end-of-life (EOL) criteria, (30% or 20% fade in rated capacity).
The sets of cells used in this paper are shown in the Table. 1. The selected datasets, which are related to three distinct operating conditions (differing in temperature and CC discharge level), are used to test the generalization capabilities of the developed algorithm.

Table 1: Reference sets of cells and relative test conditions from NASA Ames Prognostics Center of Excellence (PCoE)[19] dataset

Cell#	**Test Temperature [$^{\circ}C$]**	**Discharge Current [A]**
B05-B06-B07-B18	24	2 (CC)
B29-B30-B31-B32	24	**4 (CC)**
B33-B34-B36	**43**	4 (CC)

3.2 HI extraction

The Li-Ion batteries degradation phenomena can be observed through different type of Health Indicators that describe the behaviour of the observables at increasing cycle of operation and aging degree. Due to the user-dependant nature of the discharge phase, in many studies, the charge curves are employed in the SOH estimation. Compared to discharging, the charging process is controlled in most practical scenarios scenarios.[20] The charging phase is stable, making it ideal for Health Indicator (HI) extraction.[21] Charging strategies are generally more standardized (CC-CV). Discharge cycles, however, vary significantly depending on the application and usage patterns.[8]
Before the HI extraction the anomalous cycles are removed by a threshold criterion based on the cut-off voltage values and the minimum value of the current. Then the data are resampled and smoothed by the Savitzky-Golay filter.[22]
The pre-processed time series are used to extract health indicators. Previous research shows how multiple features allows for obtaining better results for SOH prediction.[11] For this reason, different HIs are extracted from the tree available observables: current, voltage and temperature.
The HIs used in this study can be grouped based on the observable from which they are extracted.

- Voltage based: with the increasing degradation, the speed at which the terminal voltage reaches the charging cut-off voltage accelerates.Based on this trend five Indicators are carried out from the voltage curves: Equal Time Voltage Variation (ETVV); Equal Voltage Time Variation (EVTV);[13] Constant voltage duration;[9] Voltage to Charge duration (CV/C);[9] peacks tracking of the Incremental Capacity Analysis (ICA) curve.[23]

DOI: 10.13009/EUCASS2025-653

- Current based: the duration of the Constant Current mode has a decreasing trend at an increasing degree of degradation. Based on this trend three Indicators are carried out from the current curves: Equal Time Current Variation (ETCV);[13] Constant Current duration;[11] Constant Current to Charge duration (CC/C).[9]
- Temperature based: due to the aging effect the internal resistance increase, reducing thermal stability. This phenomenon is evident in the fact that the temperature peak is reached more quickly as degradation progresses. For this reason the temperature peak time (TPT) is selected as a health indicator.[11]

3.3 HI selection

3.3.1 Correlation Analysis

The Pearson correlation coefficient is used in this study to analyse the relationship between the extracted HIs with the SOH. Due to the definition of the SOH as the ratio between the maximum available capacity (change over the cycles) and the nominal capacity (capacity at the beginning of life), the correlation between the measured capacity and HIs are evaluated for each cell in the reference dataset.
The results, depicted in Figure 1, exhibit how all the indicators are well linearly correlated with the capacity, showing a Pearson correlation coefficient >0.6, for the different cell of the dataset. An exception is the CV duration indicator for the dataset tested with a test temperature of $43°C$. This result allows the efficient solution of regression problems, which permits the estimation of the SOH starting from the extracted HIs.

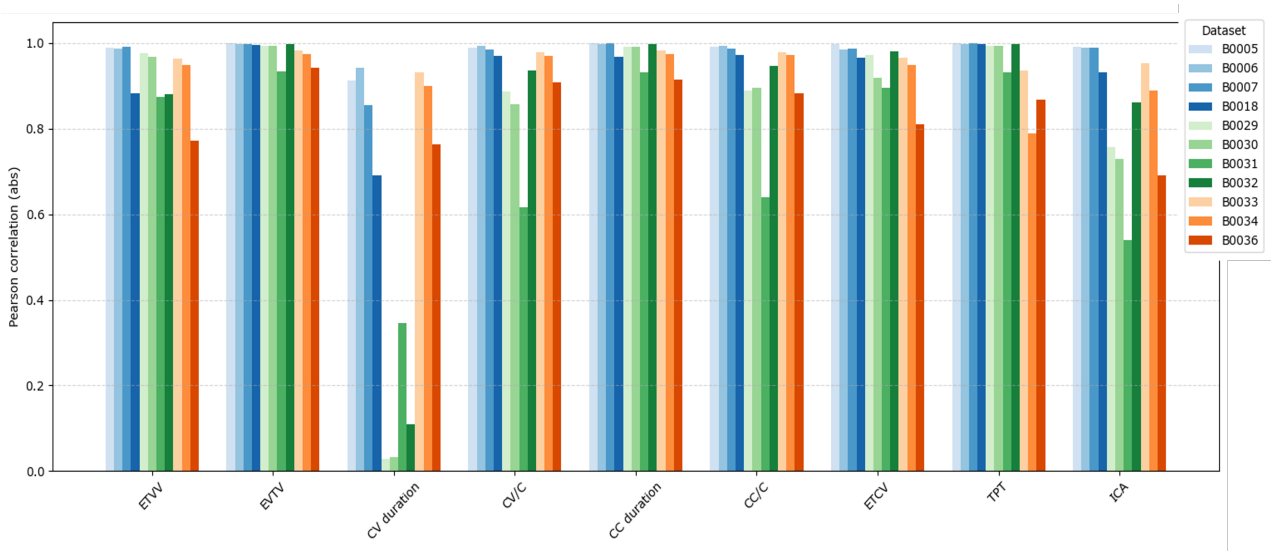

Figure 1: Comparison of Pearson correlation coefficients for different HIs across various cell sets.

3.3.2 Feature Importance

To understand how the different HIs contribute to the SOH estimation and select an optimal set of features, the capabilities of the Random Forest algorithm to assign an importance score to each feature during the training phase are used. The sum of all the scores is equal to one.
A cross-validation analysis is performed considering one cell for the dataset: B0005, B0030, B0033. Two of the three cells are used to train the RF and determine the importance of each indicator, and the third one is used to test the algorithm. The results of the feature importance carried out by the cross-validation test are shown in Figure 2 using a heat map. It is possible to observe that the importance of the indicators has a high variation when the dataset composition varies. This result indicates that the direct use of the indicators poses limitations to generalisation capabilities during the inference phase. Thus, it is not possible to select an optimal and general set of indicators that can be used in different operational conditions.
Moreover, the use of more than one HI extracted from the observables as input to a regression model can lead to redundant information, causing the occurrence of overfitting problems. For this reason, a PCA is performed to reduce

DOI: 10.13009/EUCASS2025-653

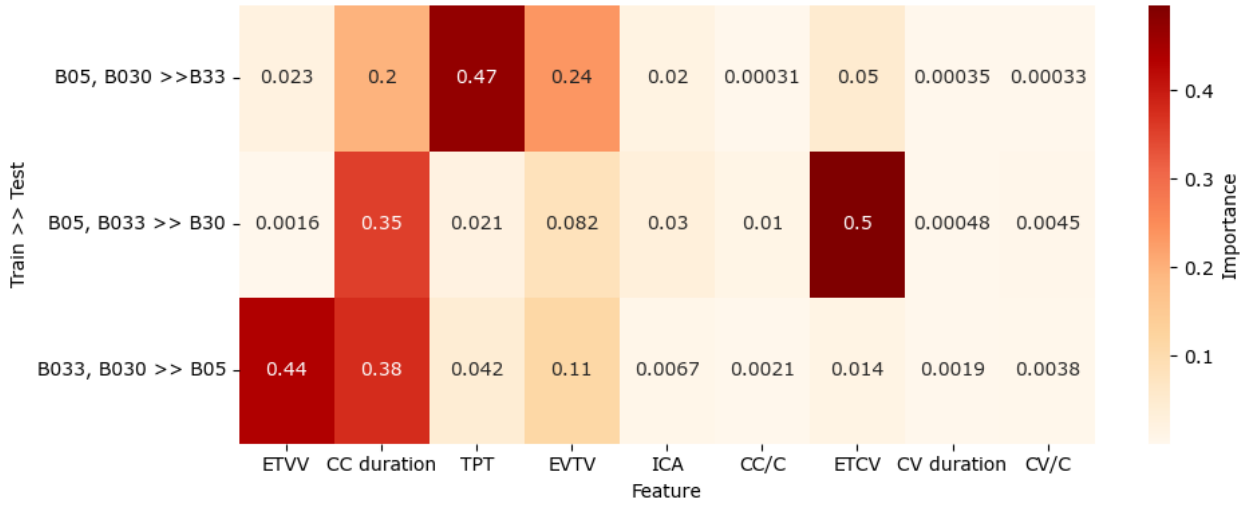

Figure 2: Feature importance cross-validation results for the extracted health indicators

the dimensionality of the dataset, obtaining a set of uncorrelated features. Each characteristic is first normalized in the range [0,1], and then the first five principal components are extracted. With the same approach described before, the cross-validation test is performed on the principal components, and the results are reported in Figure 3. In this case, it is possible to observe how the importance is totally covered by the first principal component, which remains invariant across the considered datasets. This result allows a univocal selection of the most representative indicator in different scenarios.

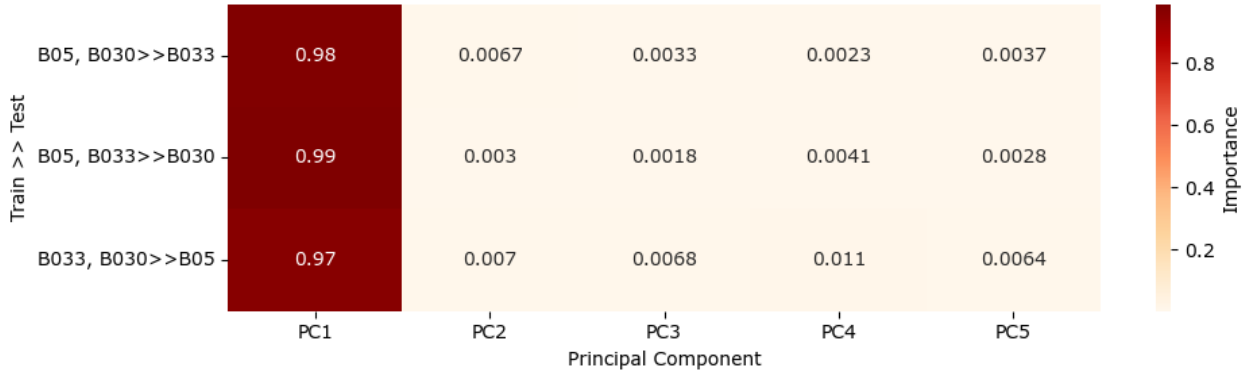

Figure 3: Feature importance cross-validation results for the Principal Components

In the cross-validation analysis, the RF algorithm is trained and used to estimate the SOH relative to the test dataset. A comparison of the results obtained using all the indicators and the principal components is reported in Table 2 in terms of Determination Coefficient R^2, and Mean Absolute Error (MAE).[6] The application of PCA improves the already good results obtained when using all the features. Specifically, it leads to a higher R^2, meaning that the model explains a greater proportion of the variance in the target variable, and a lower MAE, indicating that the average magnitude of the prediction errors is reduced.
Furthermore, leveraging the high level of correlation, it is possible to conclude that between the HIs there is a stable relation, also when different sets of cells are considered. This observation allows the PCA techniques to be used in real-time conditions using the same transformation, also when the operative conditions vary.

3.4 SOH estimation

To test the efficacy of the proposed pre-process approach, involving the principal components of the extracted HIs, a Feedforward Neural Network is employed for SOH estimation. A FNN with three hidden layers (128, 64, 32 neurons) is used to model complex patterns in the data. ReLU activation and a small dropout rate help improve generalization,

DOI: 10.13009/EUCASS2025-653

Table 2: Cross-validation performance comparison between health indicators and principal components. The *Diff %* columns shows the percentage improvement in the given metrics when utilizing principal components over health indicators.

Test	R^2 **All HIs**	R^2 **PCs**	R^2 **Diff %**	**MAE All HIs**	**MAE PCs**	**MAE Diff %**
B05	0.9249	0.9758	5.21	0.0258	0.0230	12.17
B30	0.9049	0.9204	1.68	0.0157	0.0134	17.16
B33	0.9204	0.9327	2.33	0.0205	0.0189	8.46

while the Adam optimizer ensures stable and efficient training. The model was trained with a low learning rate and (Minimum Squared Error) MSE loss, suitable for regression tasks.
The selected dataset is divided in three parts: training, validation and test. Each subset is chosen to test the generalization capability of the algorithm in the estimation of the SOH, in different operational conditions. For this reason, the training, validation and test data are respectively composed by data coming from the three different test profiles. In particular, the training set (64% of the dataset) consists of B0005, B0006, B0007, B0018 cells; the validation set (16% of the dataset) is composed of B0029, B0030, B0031, B0032; B0033 cell is used for the test (20% of the dataset).
For each dataset, the HIs are extracted, and the PCA is performed to obtain a more representative dataset. In particular, only the first principal component is considered as the input of the FNN. The results of the training and validation are reported in Figure 4, where the loss function behaviour are depicted. The figure illustrates the training and validation MSE loss over 160 epochs. The training and validation curves remain close, with only a slight gap between, suggesting that the model maintains strong generalization capabilities without signs of overfitting: the validation loss does not increase, a strong indicator that the model remains robust across epochs. As already mentioned, the validation dataset comes from different operational conditions compared to the training set. Despite this domain shift, the validation loss remains low and stable throughout the training, suggesting that the model is able to generalize effectively even under varying conditions.

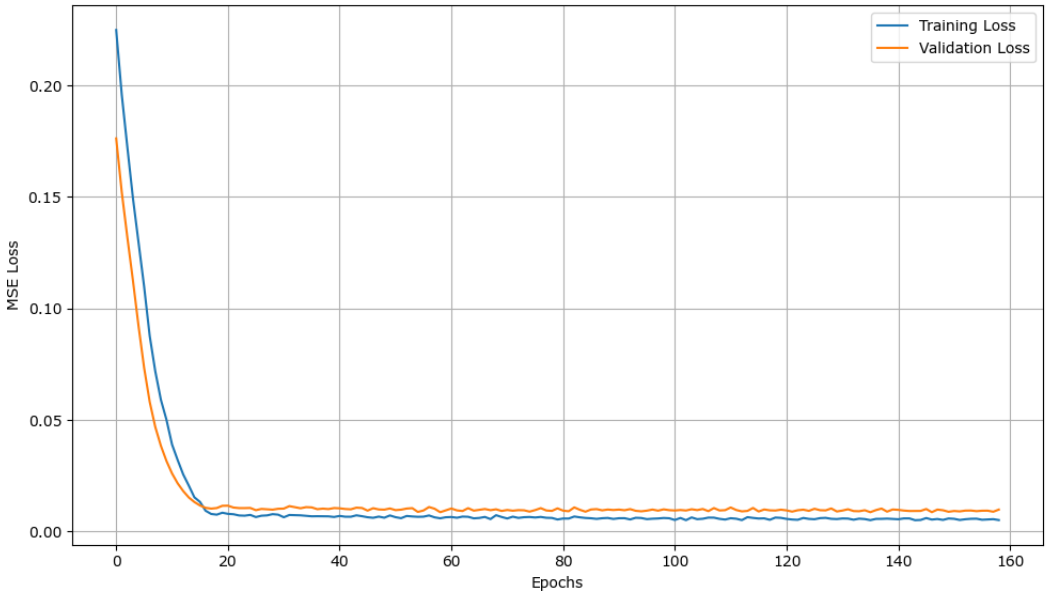

Figure 4: MSE loss function for training and validation of the feedforward network over 160 epochs

The test dataset is then used to evaluate the performances of the trained neural network. To test the pre-processing approach based on the PCA, the linear transformation used to evaluate the first principal component of the HIs extracted from the B0005 cell is used to transform (at each cycle) the HIs extracted from the B0033 cell (test).
The results of the test are showed in Figure 5. The plot compares the true SOH values with the predictions made by the FNN model across multiple charge-discharge cycles. Overall, the model successfully captures the degradation trend throughout the entire cycle range. The predictions closely follow the real values. Despite the different test conditions of the test dataset, the model continues to track the trend consistently.

DOI: 10.13009/EUCASS2025-653

The performance of the model is evaluated by R^2 and MAE metrics: R^2 score of 0.94947, indicating that it explains nearly 95% of the variance in the true SOH value; MAE is 0.0143, suggesting that, on average, the predictions have a very low deviation with respect to the actual values.

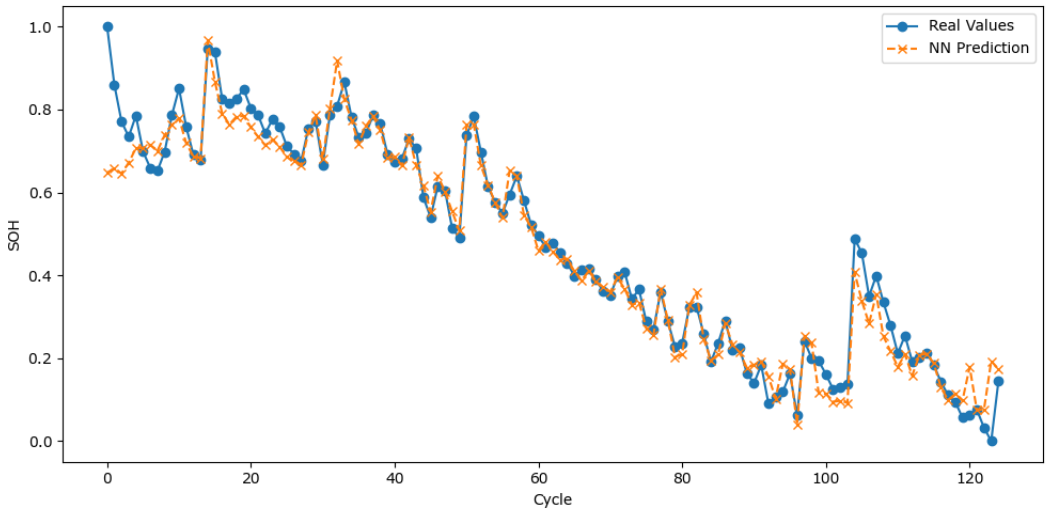

Figure 5: Comparison between true and estimated SOH values by the FNN model over multiple cycles.

4. Conclusion

This work proposes a data-driven framework for evaluating the State Of Health of lithium-ion batteries under different operating conditions. Using the NASA prognostic centre dataset as a reference, three sets of cells were selected from different experimental conditions. A set of nine health indicators was extracted from directly measurable observables of the battery during the charge phase.
A correlation analysis was performed, showing a high level of correlation between the indicators and capacity. To analyse the stability of the indicators across different test profiles, a cross-validation test was performed, leveraging the feature importance of the Random Forest. This test shows high variability in the HIs in order to represent degradation trends at various operating conditions.
Using a pre-processing procedure based on Principal Component Analysis, the degradation behaviour of the Li-ion battery is optimally captured through dimensionality reduction of the nine indicators. Cross-validation tests carried out considering only the first principal component demonstrate the high generalization capability of each dataset, improving accuracy with minor computational effort.
Finally, a feedforward neural network was trained, validated and tested considering different operating profiles, demonstrating high generalization capabilities in SOH estimation.
Future work will focus on extending the methodology to more complex operational profiles, including partial curve usage, which better reflects real mission scenarios. Particular attention will be given to handling challenges typical of space applications, such as missing data and anomalous measurements. Additionally, the algorithm will be further validated on heterogeneous datasets acquired under varying operational conditions, in order to assess its generalizability and robustness.

5. Acknowledgments

The work presented in this paper is part of an industrial PhD program co-funded by Thales Alenia Space Italia S.p.A. and by the Italian PNRR, under the M4C2 "Dalla Ricerca all'Impresa", Investimento 3.3 "Introduzione di dottorati innovativi che rispondono ai fabbisogni di innovazione delle imprese e promuovono l'assunzione dei ricercatori dalle imprese" (ref. D.M. n. 117/23), CUP: B53C23001270004.

DOI: 10.13009/EUCASS2025-653

References

[1] Htet Aung, Jing Jun Soon, Shu Ting Goh, Jia Min Lew, and Kay-Soon Low. Battery management system with state-of-charge and opportunistic state-of-health for a miniaturized satellite. *IEEE Transactions on Aerospace and Electronic Systems*, 56(4):2978–2989, 2019.

[2] Jiayi Wang and Xin Wen. Research status and progress of fault diagnosis technology for spacecraft. *Aero Weaponry*, 5:71–76, 2016.

[3] Yanqiu Xiao, Jishu Wen, Lei Yao, Jie Zheng, Zhanpeng Fang, and Yongpeng Shen. A comprehensive review of the lithium-ion battery state of health prognosis methods combining aging mechanism analysis. *Journal of Energy Storage*, 65:107347, 2023.

[4] Qi Zhao, Xiaoli Qin, Hongbo Zhao, and Wenquan Feng. A novel prediction method based on the support vector regression for the remaining useful life of lithium-ion batteries. *Microelectronics Reliability*, 85:99–108, 2018.

[5] Bin Yu, Lei Yao, and Tao Zhang. Residual life prediction of satellite lithium-ion batteries in orbital environment. In *2018 International Conference on Sensing, Diagnostics, Prognostics, and Control (SDPC)*, pages 125–130. IEEE, 2018.

[6] Fujin Wang, Zhi Zhai, Bingchen Liu, Shiyu Zheng, Zhibin Zhao, and Xuefeng Chen. Open access dataset, code library and benchmarking deep learning approaches for state-of-health estimation of lithium-ion batteries. *Journal of Energy Storage*, 77:109884, 2024.

[7] Dengfeng Zhang, Weichen Li, Xiaodong Han, Baochun Lu, Quanling Zhang, and Cuimei Bo. Evolving elman neural networks based state-of-health estimation for satellite lithium-ion batteries. *Journal of Energy Storage*, 59:106571, 2023.

[8] Iacopo Marri, Emil Petkovski, Loredana Cristaldi, and Marco Faifer. Comparing machine learning strategies for soh estimation of lithium-ion batteries using a feature-based approach. *Energies*, 16(11):4423, 2023.

[9] Muyao Wu, Yiming Zhong, Ji Wu, Yuqing Wang, and Li Wang. State of health estimation of the lithium-ion power battery based on the principal component analysis-particle swarm optimization-back propagation neural network. *Energy*, 283:129061, 2023.

[10] Yanru Yang, Jie Wen, Yuanhao Shi, and Jianchao Zeng. State of health prediction of lithium-ion batteries based on the discharge voltage and temperature. *Electronics*, 10(12):1497, 2021.

[11] Lewis Driscoll, Sebastián de la Torre, and Jose Antonio Gomez-Ruiz. Feature-based lithium-ion battery state of health estimation with artificial neural networks. *Journal of Energy Storage*, 50:104584, 2022.

[12] Yuchen Song, Datong Liu, Yu Peng, Chen Yang, and Wei Wu. Self-adaptive indirect health indicators extraction within prognosis of satellite lithium-ion battery. In *2017 Prognostics and System Health Management Conference (PHM-Harbin)*, pages 1–7. IEEE, 2017.

[13] Datong Liu, Yuchen Song, Lyu Li, Haitao Liao, and Yu Peng. On-line life cycle health assessment for lithium-ion battery in electric vehicles. *Journal of cleaner production*, 199:1050–1065, 2018.

[14] Leily Sheugh and Sasan H Alizadeh. A note on pearson correlation coefficient as a metric of similarity in recommender system. In *2015 AI & Robotics (IRANOPEN)*, pages 1–6. IEEE, 2015.

[15] Hervé Abdi and Lynne J Williams. Principal component analysis. *Wiley interdisciplinary reviews: computational statistics*, 2(4):433–459, 2010.

[16] Reza Iranzad and Xiao Liu. A review of random forest-based feature selection methods for data science education and applications. *International Journal of Data Science and Analytics*, pages 1–15, 2024.

[17] Matt W Gardner and Stephen R Dorling. Artificial neural networks (the multilayer perceptron) - a review of applications in the atmospheric sciences. *Atmospheric environment*, 32(14-15):2627–2636, 1998.

[18] Frank Emmert-Streib, Zhen Yang, Han Feng, Shailesh Tripathi, and Matthias Dehmer. An introductory review of deep learning for prediction models with big data. *Frontiers in artificial intelligence*, 3:4, 2020.

[19] Bhaskar Saha and Kai Goebel. Battery data set. *NASA AMES prognostics data repository*, 2007.

DOI: 10.13009/EUCASS2025-653

[20] Ting Wang, Jie Yang, Hu Lei, Meirong Gu, Shulin Leng, and Yufeng Meng. State of health estimation for satellite batteries based on the charge curves. In *2021 2nd China International SAR Symposium (CISS)*, pages 1–4. IEEE, 2021.

[21] Mengda Cao, Tao Zhang, Jia Wang, and Yajie Liu. A deep belief network approach to remaining capacity estimation for lithium-ion batteries based on charging process features. *Journal of Energy Storage*, 48:103825, 2022.

[22] Ronald W Schafer. What is a savitzky-golay filter?[lecture notes]. *IEEE Signal processing magazine*, 28(4):111–117, 2011.

[23] Jiachi Yao and Te Han. Data-driven lithium-ion batteries capacity estimation based on deep transfer learning using partial segment of charging/discharging data. *Energy*, 271:127033, 2023.